Mild stress conditions during laboratory culture promote the proliferation of mutations that negatively affect Sigma B activity in Listeria monocytogenes

Guerreiro, Duarte N.; Wu, Jialun; Dessaux, Charlotte; Oliveira, Ana H.; Tiensuu, Teresa; Gudynaite, Diana

Published in:
Journal of Bacteriology

DOI:
10.1128/JB.00751-19

Publication date:
2020

Document Version
Peer reviewed version

Mild stress conditions during laboratory culture promote the proliferation of mutations that negatively affect Sigma B activity in *Listeria monocytogenes*

Duarte N. Guerreiro[a], Jialun Wu[a], Charlotte Dessaux[b], Ana H. Oliveira[c], Teresa Tiensuu[c], Diana Gudynaite[d], Catarina M. Marinho[a,e,f], Aoife Boyd[g], Francisco García-del Portillo[b], Jörgen Johansson[c], Conor P. O'Byrne[a]#

[a]Bacterial Stress Response Group, Microbiology, School of Natural Sciences, National University of Ireland Galway, H91 TK33, Ireland
[b]Laboratory of Intracellular Bacterial Pathogens, National Center for Biotechnology (CNB)-CSIC, Madrid-Spain
[c]Laboratory for Molecular Infection Medicine Sweden, Department of Molecular Biology, Umeå Centre of Microbial Research, Umeå, Sweden
[d]Molecular Microbiology Department, School of Life Sciences, University of Dundee
[e]Université do Bourgogne Franche-Conté, Dijon, France
[f]Institut National de la Recherche Agronomique, UMR Agroécologie, Dijon, France
[g]Pathogenic Mechanisms Research Group, National University of Ireland Galway, Ireland

Running title: *sigB* operon mutations increase growth under stress

#Address correspondence to Conor O'Byrne, conor.obyrne@nuigalway.ie

Abstract

In *Listeria monocytogenes* the full details of how stress signals are integrated into the σ^B regulatory pathway are not yet available. To help shed light on this question we investigated a collection of transposon mutants that were predicted to have compromised activity of the alternative sigma factor B (σ^B). These mutants were tested for acid tolerance, a trait that is known to be under σ^B regulation, and they were found to display increased acid sensitivity, similar to a mutant lacking σ^B (Δ*sigB*). The transposon insertions were confirmed by whole genome sequencing, but in each case the strains were also found to carry a frameshift mutation in the *sigB* operon. The changes were predicted to result in premature stop codons, with negative consequences for σ^B activation, independently of the transposon location. Reduced σ^B activation in these mutants was confirmed. Growth measurements under conditions similar to those used during the construction of the transposon library revealed that the frameshifted *sigB* operon alleles conferred a growth advantage at higher temperatures, during late exponential phase. Mixed culture experiments at 42°C demonstrated that loss of σ^B activity allowed mutants to take-over a population of parental bacteria. Together, our results suggest that mutations affecting σ^B activity can arise during laboratory culture because of the growth advantage conferred by these mutations under mild stress conditions. The data highlight the significant cost of stress protection in this food-borne pathogen and emphasise the need for whole genome sequence analysis of newly constructed strains to confirm the expected genotype.

Importance

In the present study we investigated a collection of *Listeria monocytogenes* strains that all carried *sigB* operon mutations. The mutants all had reduced σ^B activity and were found to have a growth advantage under conditions of mild heat stress (42˚C). In mixed cultures these mutants outcompeted the wildtype when mild heat stress was present but not at an optimal growth temperature. An analysis of 22,340 published *L. monocytogenes* genome sequences found a high rate of premature stop codons present in genes positively regulating σ^B activity. Together the findings suggest that the

occurrence of mutations that attenuate σ^B activity can be favoured under conditions of mild stress, probably highlighting the burden on cellular resources that stems from deploying the general stress response.

Introduction

Listeria monocytogenes is the causative agent of listeriosis, which can sicken immunocompromised individuals and pregnant women and is associated with a high mortality rate (typically 25-30%) (1, 2). *L. monocytogenes* is ubiquitous in the environment (3) partly due to its ability to survive and grow in a wide range of harsh conditions, such as low pH, high osmolality (4) and elevated concentrations of bile salts (5). This robustness is partly under the control of the stress-inducible sigma factor sigma B (σ^B), which is responsible for the upregulation of a regulon composed of approximately 300 genes (6, 7). σ^B also plays a role in establishing infections, as it is necessary for *L. monocytogenes* survival in the gastrointestinal tract (8) and it contributes to the regulation of the internalin genes *inlA* and *inlB* that are required for host cell invasion (9).

In *Bacillus subtilis*, σ^B is regulated by a signal transduction pathway that is primarily encoded in the polycistronic *sigB* operon, which comprises eight genes, *rsbR*, *rsbS*, *rsbT*, *rsbU*, *rsbV*, *rsbW*, *sigB* and *rsbX* (10). In *L. monocytogenes* two additional genes, *mazE* and *mazF*, are located upstream of *rsbR* are also co-transcribed with this operon (11). The σ^B signal transduction pathway has been well studied in *B. subtilis,* where the main components of the system are all conserved and share a high degree of similarity with their *L. monocytogenes* counterparts (12). In the absence of stress the anti-sigma factor RsbW sequesters σ^B, blocking its interaction with RNA polymerase (13, 14). Upon encountering environmental or starvation stress an unknown signal is detected and integrated by the stressosome, a supramolecular complex composed of RsbR, RsbS and RsbT (15-18), as well as a number of RsbR paralogues (Lmo0161, Lmo0799, Lmo1642 and Lmo1842) (19, 20). This triggers the serine-threonine kinase activity of

RsbT, resulting in the phosphorylation of RsbR and RsbS and subsequent release of RsbT from the stressosome (21, 22). Once free, RsbT interacts with RsbU activating its serine phosphatase activity, which in turn results in the dephosphorylation of the anti-anti-sigma factor RsbV. The anti-sigma factor RsbW, which is also a serine kinase, possesses a higher affinity with the non-phosphorylated RsbV than σ^B, resulting in the sequestration of RsbW by RsbV and the release σ^B (23), allowing it to interact with RNA polymerase and instigate transcription of the σ^B regulon.

Several studies, both in *L. monocytogenes* and *B. subtilis*, have shown that mutations constructed within the *sigB* operon result in reduced σ^B activity as a consequence of impaired signal transduction through this pathway (21, 24-28). Although the main elements of the signal transduction pathway from the stressosome to σ^B is well described, the nature of the signals detected and the molecular mechanisms involved in the transduction of these signals are still largely unknown. Paradoxically a number of studies have reported that loss of *sigB* can result in a faster growth rate under some culture conditions. In a chemically defined medium with limiting glucose mutant strains lacking either *sigB, rsbV* or *rsbT* grow faster at 37°C than the WT (29). At 3°C a growth advantage has also been reported for a *sigB* mutant strain in complex medium (30). In the presence of sub-lethal doses of blue light, mutant strains lacking σ^B show improved growth in both liquid and solid complex media (31). These findings suggest that deploying the σ^B-controlled general stress response can under some conditions impose a cost on cells that results in a reduced growth rate.

In an attempt to develop a better understanding of the factors that influence stress sensing via the stressosome we focussed on a set of transposon mutant strains in *L. monocytogenes* EGD-e that were previously suggested to have altered σ^B activity (32). In their study, Tiensuu and colleagues discovered that *L. monocytogenes* forms distinct rings in soft agar plates when exposed to cycles of light and darkness, a phenotype that is mediated by σ^B and requires the action of RsbL (also known as Lmo0799), a

121 stressosome-associated RsbR paralogue that acts as a blue-light sensor (19). The
122 authors described the isolation of several transposon mutant strains that failed to
123 produce these rings in response to oscillating cycles of light ("ringless" phenotype) and
124 suggested that the genes carrying the transposon insertions could be involved in
125 modulating σ^B activity. The present study focussed on this collection on mutant strains
126 in the expectation that the mutated genes might give new insights into the mechanisms
127 that lead to the activation of σ^B in response to stress and potentially into the nature of
128 the stress signals detected.
129
130
131 During the preliminary stages of the present study whole genome sequencing (WGS)
132 was used to confirm the location of the transposon insertions. While confirming the
133 presence of the transposons it also revealed the presence of distinct frameshift
134 mutations in the *sigB* operon in each of the ringless strains. This suggested a simpler
135 explanation for the ringless phenotype of the transposon mutant strains; namely that the
136 *sigB* operon alleles reduced σ^B activity which in turn compromised the "ring" formation.
137 The emergence of mutations in the *sigB* operon of *L. monocytogenes* during laboratory
138 culture has been reported in a number of other studies (28, 31, 33-35). It has been
139 suggested that the occurrence of mutations impairing σ^B function might be particularly
140 associated with loss of surface proteins (36). However, the selective pressure driving
141 the emergence of these alleles is unknown. Here, we investigated the properties of
142 these *sigB* operon mutant strains to determine whether σ^B activity was affected and
143 whether that affected their fitness. The frameshift alleles that arose in the *sigB* operon of
144 these strains were associated with reduced acid tolerance, as well as a marked
145 reduction in σ^B activity. Furthermore, in the presence of mild heat stress the mutations
146 produced a fitness advantage in mixed populations with WT bacteria that was
147 qualitatively similar to that seen in a *sigB* deletion mutant strain. Together, these
148 observations suggest that loss of σ^B activity can confer a growth advantage under
149 conditions used routinely during laboratory culture of *L. monocytogenes*. We propose
150 that this effect is responsible for the common emergence of mutations in the *sigB*

operon under laboratory conditions, and that this finding has important implications for researchers studying any phenotypic properties of this pathogen.

Results

"Ringless" transposon mutants display acid-sensitive phenotypes.

Five "ringless" transposon mutant strains from the study of Tiensuu *et al.* (A4:E8, C10:A8, C14:C12, D9:B6 and D2:C10 (32). Herein renamed as 1RsbS (H23R), 2RsbU (E103K), 3RsbS (H23R), 4RsbV (E42R), 5RsbV (R47Y), respectively) were selected to investigate the possible effects of these insertions on the regulation of σ^B activity in *L. monocytogenes* EGD-e (Table 1 and 2). These "ringless" mutant strains were first reconfirmed to be defective for ring formation (data not shown), a phenotype exhibited on soft agar media in response to 12 hour cycles of light and dark and known to be under σ^B control (32) (Table 1). Since σ^B plays an important role in acid tolerance we reasoned that transposon mutations influencing σ^B activity would also lead to an altered acid resistance phenotype. To investigate this the 5 "ringless" mutant strains were tested for their ability to withstand a challenge at pH 2.5 and compared to the WT (EGD-e) and two control strains that harbour a transposon insertion but still retained the "ring" phenotype (B14:A6 and B15:E2) (32). The WT and the 2 ring-forming strains behaved similarly in this assay, showing high resistance to lethal acidic conditions, while a mutant strain lacking σ^B (Δ*sigB*) was exquisitely sensitive to acid, showing significantly decreased viable counts at 30 min and no viable counts at 60 min (Fig. 1). The "ringless" transposon mutant strains all displayed a significant increase in acid sensitivity compared to the ring-forming WT and ring-forming control strains. These data strongly suggested that σ^B activity was compromised in these strains.

The "ringless" transposon mutants harbour secondary mutations in the *sigB* operon conferring a reduced σ^B activity.

To assess whether additional mutations could be present in the transposon mutant strains displaying the ring and "ringless" phenotype, we performed WGS on each of

them. The location of the transposon insertions was found to be identical to those described by Tiensuu *et al.* (32) for eight of the strains tested (Table 2). However there were three exceptions; the *loci* reported to carry the transposon insertions in strains 1RsbS (H23R) (*lmo0040*), 2RsbU (E103K) *(lmo0124*) and 4RsbV (E42R) (*lmo0101*) were somewhat different in the WGS analysis that we performed (Table 2). This difference is likely due to the different methods used to determinate their position in the two studies.

An analysis of the genome sequences for single nucleotide polymorphisms (SNPs) revealed that all eleven of the "ringless" mutant strains had mutations in the *sigB* operon. Specifically, either the *rsbS*, *rsbU* or *rsbV* genes carried frameshift mutations that were predicted to result in deeply truncated versions of the corresponding protein products (Fig. 2 and Table 2). Six of the transposon mutant strains carried the same mutant allele in the *rsbS* gene, a four nucleotide insertion resulting in a premature stop at codon 38 (H23R; Table 2). The other five mutant strains all carried unique frameshift alleles in *rsbU*, *rsbS*, or *rsbV* (Table 2). The two ring-forming control strains selected for our study (B14:A6 and B15:E2) showed no mutation in any of the *sigB* operon genes. Based on the known functions of the proteins encoded by the *sigB* operon it seemed likely that these mutations, rather than the transposon insertions, were responsible for both the "ringless" and acid-sensitive phenotypes.

To investigate this further we focused attention on strain 3RsbS (H23R), predicted to express a truncated RsbS protein, since the loss of ring formation in this transposon-carrying strain was partially complemented in the study by Tiensuu et al. by providing the gene affected by the transposon insertion (*lmo0596*) *in trans* (32). The complementation suggested that the transposon insertion was responsible for the ringless phenotype, rather than the SNP in the *rsbS* gene, which we now suspected to be the principal cause of the phenotype. The WGS analysis revealed that the transposon was located 186 bp upstream from the start codon of *lmo0596* and 40

upstream from the divergently transcribed gene *sreB*, which encodes a sRNA S-adenosylmethionine (SAM) riboswitch (37). We reasoned that if disruption of either *lmo0596* or *sreB* was responsible for the ringless phenotype then deletion of either gene should produce a similar phenotype. Deletion of neither gene produced a ringless phenotype, whereas loss of *sigB* produced the expected loss of ring formation (Fig. S1 A). If the transposon impacted σ^B activity through effects on either *lmo0596* or *sreB* then loss of these genes might be expected to affect acid tolerance, another highly σ^B-dependent phenotype. However deletion of neither gene produced any detectable effect on survival at pH 2.5, unlike the Δ*sigB* mutation, which produced an acid sensitive phenotype (Fig. S1 B & C). Similarly, if the transposon insertion in this strain was affecting σ^B activity via an effect on these genes the transposon might be expected to affect the transcription of one or both genes. RT-qPCR was used to measure the relative levels of *lmo0596* and *sreB* transcription in the transposon carrying strain 3RsbS compared to the wild-type, the Δ*sigB* mutant, and two other transposon-carrying strains (the ring forming strain B12:A6 and the ringless strain 1RsbS). The transcription of *lmo0596* was confirmed to be σ^B-dependent, as earlier suggested (38), but no difference in transcription was observed between the 3RsbS and 1RsbS strains, which carry transposon insertions in completely separate *loci* (Fig. S1 D; Table 2). Neither was *sreB* transcription affected by the presence of the transposon (Fig. S1 D). Finally, the deletion of *lmo0596* had no effect on the transcription of the σ^B-dependent gene *lmo2230* suggesting that this gene does not play a role in regulating σ^B activity (Fig. S1 E). Taken together these results suggest that the transposon insertion in strain 3RsbS is not responsible for the observed ringless phenotype in 3RsbS (H23S) and we therefore we conclude that the altered phenotype in the 3RsbS (H23R) transposon mutant is solely due to the frameshift mutation in *rsbS*, and suggest that the *sigB* operon mutations in the other strains are most likely responsible for their σ^B-related phenotypes too.

To investigate this further σ^B activity was measured in these strains using a previously described transcriptional reporter that fuses the highly σ^B-dependent promoter of

lmo2230 (annotated as a putative arsenate reductase) to the enhanced green fluorescent protein gene (*egfp*) (39). This reporter was integrated into the genome, upstream of the original promoter of *lmo2230*, of the WT, the Δ*sigB* mutant strain and seven of the transposon insertion strains, including five "ringless" and two ring-forming control strains. Fluorescence was recorded by fluorescence microscopy following growth to stationary phase at 37°C, a condition where σ^B is known to be highly active (24, 39). As expected the Δ*sigB* mutant strain had almost no detectable fluorescence while the WT and ring-forming transposon control strains (B14:A6 and B15:E2) produced a strong fluorescent signal (Fig. 3 A & B). In contrast the "ringless" strains that carried mutations in *rsbS*, *rsbU* or *rsbV* all produced a greatly reduced fluorescence signal, albeit not as low as the Δ*sigB* deletion mutant strain. Western-blotting was used to determine the levels of eGFP protein in the reporter strains under the same growth conditions. The results confirmed what was observed microscopically; very low levels of eGFP expression in the Δ*sigB* mutant strain and in the strains harbouring *sigB* operon mutations, but not in the WT or ring-forming transposon mutant strains (Fig. 3 C & D). These data confirmed that σ^B activity was reduced in the strains that displayed both an acid-sensitive and ringless phenotype. The most parsimonious explanation for these observations is that the *sigB* operon alleles in the "ringless" mutant strains were directly responsible for the reduced σ^B activity and associated phenotypes, especially since defined mutations in these genes, in both *L. monocytogenes* and *B. subtilis*, have previously been shown to result in reduced σ^B activity (14, 27-29, 31, 36, 40, 41). Moreover, the ring-forming transposon mutant strains used as controls exhibited similar phenotypes to the WT strain. It is highly unlikely therefore that the transposons themselves were responsible for any of the phenotypes detected in these strains.

The *rsbS* frameshift results in a polar effect on *rsbT*.

The *sigB* operon has the gene order *mazEF-rsbRSTUVW-sigB-rsbX,* with a σ^A promoter located upstream from *rsbR* and a σ^B-dependent promoter upstream from *rsbV* (Fig. 2). Mutations in *rsbS*, *rsbU* and *rsbV* could potentially produce polar effects on downstream genes further impacting the pathway leading to σ^B activation. To address this western-

blots were performed using polyclonal antibodies against RsbT and σ^B on each of the strains. The levels of RsbT were markedly reduced in the "ringless" strains carrying the *rsbS* H23R allele but were similar to the WT in the strains carrying either the *rsbU* or *rsbV* frameshift alleles (Fig. 4 A). In contrast the levels of σ^B protein were similar in all the strains (with the exception of the Δ*sigB* mutant strain) (Fig. 4 B). These data show that the effects of the *rsbU* and *rsbV* frameshift alleles on σ^B activity are probably directly caused by the loss of these proteins. The *rsbS* frameshift allele affects the expression of RsbT, suggesting that these genes may be translationally coupled and that the loss of σ^B activity in this strain likely arises through a loss of both stressosome-associated proteins.

Reduced σ^B activity confers increased growth rate at higher temperatures.

Since the procedure for generating the transposon mutants involved an incubation step at a range of different temperatures (32, 42) we hypothesised that *sigB* operon mutations might arise if the mutant strains had a growth advantage in these conditions. To assess this cultures of the WT, Δ*sigB* mutant strain, one of the "ringless" mutant strain (designated 2RsbU (E103K)) and a ring-forming transposon mutant strain control (B14:A6) were grown at 30°C, 37°C, 40°C and 42°C and their growth rates determined (Fig. 5). At 30°C there was no significant effect of the genotype on the growth rates, whereas at the higher temperatures the "ringless" mutant strains lacking *sigB* or with an *rsbU* frameshift allele (E103K) exhibited a slight increase in the growth rate. At 42°C these two mutant strains grew noticeably faster than the WT and ring-forming control B14:A6 strains, especially as the cultures approached stationary phase between 4 to 7 h after inoculation (Fig. 5 D). This finding raised the possibility that mutations arising spontaneously in the *sigB* operon could be selected for at higher temperatures because of a growth advantage relative to WT cells possibly due to the reduced σ^B activity.

To further examine this possibility we performed mixed culture competition experiments to determine if the growth rate advantage would enable the Δ*sigB* and *sigB* mutants to

outcompete the WT during growth at elevated temperatures. Cultures were prepared that mixed the WT with the Δ*sigB* mutant strain or the "ringless" *rsbU* mutant strain (2RsbU (E103K)) or the ring-forming control strain B14:A6 mutant strain in a ratio of 1000:1 (WT:mutant). Cultures were grown over a period of 5 days, with a daily passage into fresh medium and dilutions were plated daily onto BHI agar to determine the relative proportion of each strain. The erythromycin resistance of the transposon containing strains was used to differentiate the WT from mutant strains, while a difference in the colony colour was used to discriminate the WT and the Δ*sigB* mutant strain, as described in the materials and methods. When the mixed cultures were grown at 42°C the "ringless" mutant strains carrying the *rsbU* frameshift allele accumulated steadily, reaching approximately 50% of the population after 5 days (Fig. 6 A). In contrast the ring-forming control strain did not accumulate in the culture over this period (Fig. 6 B). At 42°C the Δ*sigB* mutant strain accumulated within the population, dominating it (80:20) by the end of 5 days. However at 30°C, where this growth advantage was absent (Fig. 5 A), the Δ*sigB* mutant strain failed to fully dominate the population, reaching approximately 10% by the end of 5 days (Fig. 6 D). When cultures were mixed 1:1 and grown at 42°C the advantage was less evident for the "ringless" strain carrying the *rsbU* allele but the Δ*sigB* mutant strain still dominated the WT under these conditions (Fig. S2). When the WT was started as the minority strain (1:1000) in these competition assays it failed to emerge as the dominant population when competed against any of three mutant strains tested (Fig. S2 E-G). Overall the data suggest that strains with reduced σ^B activity can accumulate in a mixed population when the growth temperature is elevated.

Loss of *rsbX* results in reduced competitiveness.

The observations above suggest that a growth advantage arises in strains with reduced σ^B activity when a mild heat stress is present. A corollary of this conclusion is that increased σ^B activity might be expected have a negative effect on growth and competitiveness. In the current model of σ^B regulation in *L. monocytogenes* RsbX is believed to act as phosphatase whose function is to reset the resting state of the

337 stressosome following a stress signalling event (43, 44). Thus RsbX plays a negative
338 role in regulating σ^B activity and the loss of RsbX is expected to have produced a strain
339 with elevated σ^B activity. To investigate this, competition experiments were performed
340 with a Δ*rsbX* mutant strain to test the competitiveness of this strain relative to the WT at
341 both 30˚C and 42˚C (Fig. 7). When Δ*rsbX* was present as the minority strain (1000-fold
342 under-represented at the start of the experiment) it failed to dominate the culture over 5
343 days of passaging, regardless of the temperature (Fig. 7 A & B), although it did recover
344 its population somewhat over this period. When the WT was the minority strain it
345 outgrew Δ*rsbX* over the same time period (Fig. 7 C & F), showing that the WT had a
346 competitive advantage over the mutant strain. When the populations were equal at the
347 start of the experiment the WT tended to dominate the mixed cultures (Fig. 7 B & E).
348 This result was observed at both incubation temperatures, probably because the growth
349 of the Δ*rsbX* strain was inhibited regardless of the temperature. Overall these results
350 are consistent with the idea that mutations that increase σ^B activity produce a growth
351 disadvantage.
352
353
354 **Premature stop codons occur with a higher than average frequency in the**
355 **positive regulators of σ^B within the *sigB* operon.**
356 The occurrence of *sigB* operon mutations in this study and in other studies (28, 31, 33-
357 36) prompted us to investigate whether undocumented premature stop codons
358 (PMSCs) might be present in the *sigB* operon in genome sequences deposited in public
359 databases, so we searched for PMSCs in the *sigB* operon among 22,340 of *L.*
360 *monocytogenes* genome assemblies. The PMSC rate per 100 bp (expressed as a %
361 rate per 100 bp to normalise for gene length) for genes in the *sigB* operon that positively
362 affect σ^B activity (*rsbV*, *rsbT* and *rsbU*) was considerably higher than for genes that act
363 negatively (*rsbW* and *rsbX*). Indeed of all the genes we included in the analysis, *rsbU*
364 was found to have the highest occurrence of PMSC (Fig. 8 A & B). Unexpectedly,
365 *mazF* showed a high PMSC rate similar to *rsbV*, *rsbT* and *rsbU*. The gene *mazF*
366 encodes for an endoribonuclease, a component of a toxin/anti-toxin system along with
367 *mazE*, which is speculated to be an additional regulator for σ^B in *Staphylococcus aureus*

(45, 46) and have a positive effect in σ^B-dependent genes in *L. monocytogenes* in the presence of norfloxacin (47). The high PMSC rate in *mazF* may be associated with its putative positive regulation on σ^B thus it may also be subjected to the same selection pressure as σ^B positive regulators. Interestingly *rsbW,* which encodes the anti-sigma factor that negatively regulates σ^B activity, had no occurrence of PMSCs. As expected, essential genes such as *sigA*, which encodes the principal housekeeping sigma factor in *L. monocytogenes*, have a very low rate of PMSC occurrence, suggesting that this measure reflects the biological significance rather than just sequencing errors in the database. Interestingly, we found that the gene *inlA*, encoding for the internalin A was found to possess a very high PMSC rate per 100 bp (0.86% from a total of 4576 PMSCs found; data not shown). A previous study found that many of *L. monocytogenes* strains in lineage II possess PMSCs in *inlA* (48), for this reason we excluded this gene from Fig. 8. Interestingly, *inlB* which shares the same operon as *inlA*, also possess a high PMSC rate, although not as high as *inlA* (Fig. 8). Taken together these data indicate that within the published genome sequence data for *L. monocytogenes* there is a high occurrence of mutations that are predicted to reduce σ^B activity and low occurrence of mutations that would act to increase it.

Discussion

In this study we investigated the emergence and selection of spontaneous mutations inactivating σ^B within populations of *L. monocytogenes*. We first identified these mutations in a collection of *L. monocytogenes* “ringless” transposon mutant strains whose response to visible light was altered, a phenotype that requires both the blue light sensor RsbL and the stress-inducible sigma factor σ^B (32). One interpretation of the mutants’ behaviour was that the transposon insertions somehow influenced the signal transduction pathway leading to σ^B activation in response to light. Unexpectedly we found that, in addition to the transposon insertions, all of the “ringless” mutant strains we sequenced carried mutations in the *sigB* operon (*rsbS, rsbU* or *rsbV*), which were predicted to produce premature stop codons in the corresponding coding sequences. In addition to the “ringless” phenotype, the transposon mutant strains also exhibit reduced

399 acid tolerance and a marked decrease in σ^B activation when compared to the WT strain.
400 We conclude that the "ringless" and acid sensitive phenotypes of these mutant strains
401 are due to the presence of the *sigB* operon mutations rather than the transposon
402 insertions (32). These mutations most likely interfere with signal transduction through
403 the σ^B regulatory pathway since they are predicted to affect stressosome function
404 (*rsbS*), dephosphorylation of the anti-anti sigma factor RsbV (*rsbU,* which encodes a
405 phosphatase) or partner switching with the anti-sigma factor RsbW (*rsbV*). Indeed these
406 data provide additional genetic support for the existing model for σ^B activation in *L.*
407 *monocytogenes,* reviewed in (49, 50).
408
409
410 In previous studies, knockout deletions of the *rsbS*, *rsbV* or *rsbU* genes in both *L.*
411 *monocytogenes* and *B. subtilis* resulted in the impairment of the signal transduction and
412 reduced resistance against stress (14, 27-29, 31, 36, 40, 41). The premature stop
413 codons identified in this study do not result in the full loss of σ^B activity, since the σ^B-
414 dependent $P_{lmo2230}$::*egfp* reporter is still expressed in these transposon mutant strains
415 (Fig. 3) and this correlates with an intermediate acid tolerance phenotype, between that
416 of WT and the Δ*sigB* mutant strain (Fig. 1). It is noteworthy that no mutations were
417 detected in *sigB* itself, which could suggest that partial loss of function might be more
418 advantageous than complete loss of σ^B activity. The extent of the σ^B activity detected
419 appears to depend on which *sigB* operon frameshift allele is present. There is
420 significantly more σ^B activity present in strains carrying the frameshift allele encoding
421 RsbS-H23R than there is in the strains carrying either of the two *rsbV* frameshift alleles
422 (Fig. 3). This result suggests that loss of a functional RsbV has a greater impact on σ^B
423 activity than loss of RsbS. RsbV serves as an anti-anti sigma factor, whose role is to
424 sequester the anti-sigma factor RsbW during stress conditions, thereby releasing σ^B for
425 participation in transcription, while RsbS is an integral component of the stressosome
426 stress-sensing apparatus (16, 51). It is possible that some stress signals can still be
427 transduced through the pathway in the absence of RsbS but that this is less likely in the
428 absence of RsbV. In *B. subtilis* there is additional input into the pathway, which allows
429 energy stress to be sensed via the RsbP and RsbQ proteins, independently of the

stressosome (52). This pathway is not present in *L. monocytogenes* (29) but this does not preclude some other stressosome-independent means of transducing stress signals in this pathogen. Indeed there is evidence that even in the absence of RsbV some σ^B activation can occur in some growth conditions (40). In *B. subtilis* RsbV-independent activation of σ^B occurs at elevated temperatures (53) and in *L. monocytogenes* similar observations have been made during growth at low temperatures (40, 54). The possibility that RsbW could be regulated post-translationally, for example by proteolysis, allowing an additional layer of control over σ^B is certainly worthy of further investigation.

Emergence of mutated alleles within the *sigB* operon.

The data presented here suggest an explanation for the common detection of mutations in the *sigB* operon of *L. monocytogenes* (28, 33-36, 55), including an earlier study in our own laboratory where an *rsbV* missense mutation arose during routine subculture (31). Although the occurrence of *sigB* operon mutations has been reported by others, the mechanism(s) that drives the selection of these mutations has remained elusive. Here we show that loss of σ^B function confers a competitive advantage in conditions where sub-lethal stress (in this case heat stress) prevails. The advantage is manifested both as increased growth rate (Fig. 5) and increased competitiveness in mixed cultures (Fig. 6). Furthermore, the absence of *rsbX* which is predicted to increase σ^B activity confers a competitive disadvantage under the same conditions (Fig. 7). Since a variety of the protocols for genetically modifying *L. monocytogenes* include a step with prolonged incubation at elevated temperature (typically 40-44˚C) to prevent replication of plasmids possessing a heat-sensitive origin of replication, used in order to encourage allele integration into the chromosome (42, 56), it is possible that this provides the necessary selective pressure to select mutant strains that negatively affect σ^B activity. Previous studies have reported fast-growth phenotypes for *L. monocytogenes* mutant strains lacking σ^B in stress conditions. In the presence of inhibitory doses of blue light *sigB* mutant strains grow faster than the WT in liquid and solid media (31). In glucose-limited conditions mutant strains lacking σ^B or the positively acting regulators RsbT or RsbV were found to grow faster than the WT parent (29). A similar phenotype was observed

during growth at 3˚C (30) and in conditions of osmotic stress (57). Indeed, there is evidence in *B. subtilis* that mutant strains lacking σ^B can dominate the population in nutrient-limited chemostats (58). Taken together with the findings presented in this study, where a competitive advantage is demonstrated for mutant strains with reduced σ^B activity in mixed populations, it seems likely that this phenotype is the reason for the common emergence of mutations affecting σ^B activity during routine laboratory culture of this pathogen.

An analysis of the over 22,000 *L. monocytogenes* publically available genome assemblies revealed a high rate of premature stop codons within genes of the *sigB* operon that positively regulate σ^B activity (Fig. 8), suggesting that there is some selective pressure driving this process. It is not possible to determine precisely when these PMSCs occurred and so it is unclear at present whether these mutations arose during laboratory culture or whether they were already present in the wild isolates. It is possible that conditions other than mild heat stress can confer a growth advantage on mutant strains with reduced σ^B activity, as has been observed previously with light stress and salt stress (57, 59). In *Escherichia coli* prolonged starvation during stationary phase frequently results in mutant strains displaying a so-called GASP (Growth Advantage in Stationary Phase) phenotype and these arise as a result of reduced expression or activity of σ^S (RpoS), the sigma factor that controls the general stress response in that organism (60, 61). Indeed mutations affecting *rpoS* frequently arise during lab domestication of *E. coli* strains (62). A similar explanation has been postulated to account for these observations in *E. coli*; namely the loss of σ^S function arises when a fitness advantage accrues through the allocation of resources to growth rather than to the costly general stress response (63, 64). Thus the phenomenon we describe in this study is likely a reflection of a general biological principal where competition within populations occasionally favours the emergence of variants that have acquired a growth advantage at the expense of their ability to withstand potentially lethal stress.

σ^B deployment is a trade-off between growth and survival.

Our study raises the important questions of how and why σ^B negatively affects growth and competitiveness in mixed cultures. A number of possible, perhaps co-existing, models could account for these phenomena. Firstly, it is possible that the expression of the large σ^B regulon (approximately 300 genes), many components of which are actively involved in homeostatic and repair functions, might represent a significant energy burden on the cells. Freeing the cells from this energy burden could make more resources available for biosynthesis and growth. Secondly it is possible that there is a limited transcriptional capacity in the cell and the absence of σ^B allows the housekeeping sigma factor (σ^A) to have greater access to the RNA polymerase core enzyme, which leads to more efficient transcription of genes involved in growth-related functions. This idea has been proposed previously to account for the emergence of sigma S (*rpoS*) mutations in *E. coli* (65-67). Thirdly it is possible that σ^B actively restricts growth, perhaps to ensure that protection and repair functions have sufficient time to mitigate the damaging effects of stress. We recently provided evidence for this model as we identified a sRNA under σ^B transcriptional control (Rli47) that acts to restrict the biosynthesis of isoleucine, even when isoleucine is absent from the growth medium (68). This somewhat surprising finding could provide evidence of deliberate σ^B-controlled growth restriction. It is clear that further experiments will be needed to specifically test these possibilities and establish the basis for the fast growth phenotype associated with loss of σ^B activity.

Overall this study highlights the frequent occurrence of secondary mutations negatively affecting σ^B activity in newly constructed strains of *L. monocytogenes*. It further suggests that caution needs to be exercised by researchers to ensure that this issue does not confound the interpretation of phenotypic data, especially where temperature selection has been used during the strain construction. The availability and comparative affordability of whole genome sequencing for bacteria makes it possible to routinely sequence the genomes of newly constructed strains in order to avoid this issue and

indeed the availability of this data will make it easier to compare the behaviour of strains between groups. Finally, the study clearly illustrates the cost to the cell of deploying the σ^B-mediated general stress response; protection against stress is a resource-intensive process, but presumably the long-term survival benefits outweigh the short costs.

Materials and methods

Bacterial strains, plasmids and primers.

L. monocytogenes EGD-e and *E. coli* strains, primers and plasmids used for this study are listed on Table 1 and 3, respectively. Strains were grown in Brain Heart Infusion (BHI) broth or agar (LabM) at 37°C unless otherwise specified, at 150 rpm of constant shaking. Cells were grown for 16 h until stationary phase was reached. The following antibiotic concentrations were added to the media when required: chloramphenicol (Chl) 10 µg.mL^{-1}, erythromycin (Ery) 5 µg.mL^{-1}, tetracycline (Tet) 2.5 µg.mL^{-1} for *L. monocytogenes* mutant strains; ampicillin (Amp) 100 µg.mL^{-1} for *E. coli*.

Construction of genetically modified *L. monocytogenes*.

L. monocytogenes transposon mutant strains library was previously constructed by Tiensuu *et al.* (32). Electrocompetent cells were created as previously described (69). *L. monocytogenes* EGD-e Δ*sigB* mutant strain was constructed using a previously built shuttle vector pMAD::Δ*sigB* (68). The shuttle vector pMAD::Δ*rsbX* was generated by amplifying through PCR the *rsbX* flanking regions using primers *rsbX*-A and -B and *rsbX*-C and -D in separate reactions. Both flanks were joined together through splice overlap extension (SOE) PCR (69) using primers *rsbX*-A and -D. The resulting amplicon was digested with SalI and BglII and cloned into pMAD vector creating pMAD::Δ*rsbX*. Confirmation of the construct was carried out by PCR using primers pMAD-U and pMAD-L. pMAD::Δ*lmo0596* was constructed by digesting the artificially synthetized vector pEX-K168::Δ*lmo0596* (Eurofins Genomics) with BamHI and SalI. The digestion product, containing 300 bp both upstream and downstream of *lmo0596* open reading frame, was ligated into pMAD vector creating pMAD::Δ*lmo0596*. Its construction was

verified by PCR with primers *lmo0596*-A and *lmo0596*-B. The mutagenic vectors, pMAD::Δ*sigB*, pMAD::Δ*rsbX* and pMAD::Δ*lmo0596* were separately transformed into electrocompetent *L. monocytogenes* EGD-e. Transformants were selected from BHI agar supplemented with Ery growth at 30°C. Chromosomal integration of the vector was achieved by growing transformants at 39°C overnight in BHI supplemented with Ery. Cultures were plated in BHI agar containing the same antibiotic and X-gal (50 µg.mL^{-1}) and colonies were allowed to growth at 41°C overnight. Blue colonies were growth at 30°C overnight and 39°C for 3 hours. Serial dilutions were plated on BHI X-gal (50 µg.ml^{-1}) plates and grown at 30°C for two days. White colonies (indicating excision and loss of plasmid) were screened for erythromycin sensitivity and deletion knockouts of *sigB*, *rsbX* and *lmo0596* were checked by colony PCR using primers sigB-flank_F and sigB-flank_R, lmo0596-flank_F and lmo0596-flank_R and rsbX-flank_F and rsbX-flank_R, respectively. The σ^B reporter vector pKSV7-P$_{lmo2230}$::*egfp* (24) was transformed into electrocompetent *L. monocytogenes* transposon mutant strains. Electro-transformed colonies, were selected from BHI agar plates containing Chl and incubated at 30°C. The plasmid integration in the chromosome was achieved as previously described (24) by incubating fluorescent cells at 42°C. Plasmid's chromosomal integration occurred upstream of the original *lmo2230* promoter region of by homologues recombination. Integration was verified by PCR (using primers *egfp-lmo2230*-F integration and *egfp-lmo2230*-F integration).

Acid tolerance (pH 2.5).

Stationary phase cultures were pelleted down by centrifugation and resuspended in BHI, previously acidified with HCl 5 M until pH 2.5. Resuspensions were incubated in a water-bath at 37°C for 120 min. Samples were taken at 0, 30, 60 and 120 min, serial diluted from 10^{-7} to 10^{-2} in PBS and plated in BHI agar plates. Plates were then incubated at 37°C for 24 hours and colonies were counted. A minimum of three biological replicates were made.

Whole genome sequencing (WGS).

Transposon mutant strains genomic DNA was extracted using DNeasy® Blood & Tissue Kit (Qiagen) following the manufacturer recommendations. Purified genomic DNA was sent to MicrobesNG for WGS. The obtained trimmed reads were used for SNP identification analysis performed in Breseq (70). The transposon sequence was located in each transposon mutant strain by using the contig reads on Mauve - Multiple Genome Alignment (71). *L. monocytogenes* EGD-e (NCBI Reference Sequence: NC_003210.1; (https://www.ncbi.nlm.nih.gov/nuccore/NC_003210.1) genomic sequence was used as reference genome in both analysis.

Microscopic quantification of eGFP fluorescence.

Cells containing the eGFP σ^B-reporter (pKSV7-$P_{lmo2230}$::*egfp*) integrated in *L. monocytogenes* chromosome were grown for 16 h to stationary phase. Cultures were mixed in 1:1 volume of ice cold methanol/ethanol 1:1 (v/v) mixture and placed at -20°C for 10 min. The mixtures were centrifuged afterwards at 10,000 x *g* for 10 min at 4°C. The supernatant was removed and the pellet was resuspended in ice cold PBS and cells were further adjusted to OD_{600} of 1. Fluorescence microscopy was performed in a Nikon Eclipse E600 microscope by using a B-2A filter covering the eGFP excitation and emission wavelengths. A total of 5 images per biological replicate were taken across different fields of the slide. Images were digitally captured through a CCD camera attached to the microscope. Relative fluorescence intensities were reported after automated image processing of multiple fields with ImageJ 1.44 software (72) with appropriate manipulations as described by others (73, 74).

SDS-PAGE and Western-Blot.

The total protein fraction were extracted from stationary phase cultures grown at 37°C. Tet was added to the cultures and centrifuged at 9,000 x *g* for 15 min at 4°C. Cells were resuspended in Sonication buffer containing 13 mM Tris-HCl, 0.123 mM EDTA and 10.67 mM $MgCl_2$ adjusted to pH 8.0. Cell suspensions were digested with 1 $mg.mL^{-1}$

lysozyme (Sigma-Aldrich) for 30 min and centrifuged again. Pellets were resuspended in sonication buffer containing 1% (v/v) protease inhibitor cocktail (P2714, Sigma-Aldrich). Resuspensions were then transferred into cryotubes containing zirconia/silica beads (Thistle Scientific) and beadbeated in FastPrep®-24 at a speed of 6 $m.s^{-1}$ for 40 s twice. Lysates were centrifuged for 13000 x *g* for 30 min at 4°C and the supernatant recovered. Total protein quantification was performed through DC Protein Assay (Bio-Rad) using the manufacturer recommendations. Protein extracts were normalized to 0.8 $mg.mL^{-1}$ of total protein concentration and 12 µL of each sample was separated by SDS-PAGE (15% acrylamide/bis-acrylamide) along with the PageRuler™ Plus Prestained (Thermo Scientific). Separated protein was transferred into a Polyvinylidene difluoride (PVDF) membrane and blocked with TBS supplemented with 3% (w/v) skim milk power (Sigma). SDS-PAGE gels were further stained with GelCode® Blue Staining Reagent (Thermo Scientific) and destained with destaining solution (20% acetic acid and 10% methanol) (Fig. S3). For immunoblots, rabbit polyclonal IgG anti-GFP (FL) (Santa Cruz® Biotechnology) and rabbit polyclonal IgG anti-σ^B (40), were diluted 1:500 and 1:1500, respectively, in TBS. The rabbit polyclonal IgG anti-RsbT were diluted 1:5000 in SignalBoost™ Immunoreaction Enhancer Kit (Merck). Secondary antibodies mouse anti-rabbit IgG-HRP (Santa Cruz® Biotechnology) were diluted 1:6500 in TBS or SignalBoost™ Immunoreaction Enhancer Kit (Merck) when required. Blots were visualized on Odyssey®Fc Imaging System (LI-COR Biosciences).

Growth kinetics.

Stationary phase cells grown in BHI at 37°C of *L. monocytogenes* WT, Δ*sigB*, B14:A6 and 2RsbU (E103K) were adjusted to an OD_{600} of 0.05 and grown in BHI at 30°C, 37°C, 40°C and 42°C. OD_{600} of each culture was measured every hour for 12 hours. Growth rates were calculated by determining the slope during the transition into the stationary phase, between 4 and 5 hours at 37°C, 40°C and 42°C and between 6 and 7 at 30°C. A minimum of 3 biological replicates were made.

Competition experiments.

L. monocytogenes WT, the "ringless" 2RsbU (E103K) and ring-forming control B14:A6 were grown in BHI at 37°C for 16 hours until stationary phase was reached. Cultures were adjusted to an initial OD_{600} of 0.05 in fresh BHI in final ratios of 1:1000, 1:1 and 1000:1 of mixtures of WT with 2RsbU (E103K) and WT with B14:A6, at the indicated temperatures. Passages were made every 24 hours by diluting 1:100 into fresh BHI. Samples were taken and diluted to 10^{-7} in PBS in every passage and plated in both BHI and BHI supplemented with erythromycin to distinguish non-erythromycin resistant WT from the resistant transposon mutant strain colonies and incubated at 37°C. Colonies were counted after 24 hours of incubation. Ratios were calculated by subtracting the number of erythromycin resistant colonies to the total number of colonies. Competitions cultures of WT vs. Δ*sigB* and WT vs. Δ*rsbX* were performed as described above with the following modifications. Cultures were incubated in BHI agar plates for 24 hours at 37°C. Differences in colony morphology were used to distinguish WT from both Δ*rsbX* and Δ*sigB* strains. The colony size of Δ*rsbX* colonies was significantly smaller than the WT strain. For WT vs. Δ*sigB* competitions, BHI plates were further incubated at 30°C for 7 days and strains were distinguished by differences in colony coloration. We observed that the WT colonies showed whiter coloration in comparison with the Δ*sigB*. Confirmation of WT and Δ*sigB* mutant strain colonies were carried out through colony PCR, by amplifying the flanking regions of *sigB* (using primers *sigB*-flank_F and *sigB*-flank_R). A total of 60 colonies, 30 of each coloration were tested using MyTaq™ DNA Polymerase Kit (Bioline). WT and Δ*rsbX* mutant strain were also confirmed via the same method by amplifying the flanking regions of *rsbX* (using primers *rsbX*-flank_F and *rsbX*-flank_R) of a total of 24 colonies, 12 WT and 12 Δ*rsbX*. This method enables the WT to be distinguished from the Δ*sigB* with a precision of 98.3% and the WT from the Δ*rsbX* with 100%.

***In silico* analysis of premature stop codon (PMSC) occurrence rates.**

A DNA BLAST database was constructed for 22,340 *L. monocytogenes* genome assemblies available from NCBI database (182 complete genomes, 45 chromosomal

genomes and 22,113 assembly scaffold or contigs, accessed in July 5th 2019). DNA coding sequences of 41 genes of interest, including all 10 genes from the *sigB* operon, 2 genes immediately downstream from the *sigB* operon, 7 housekeeping genes used in Multilocus Sequencing Typing (MLST) (75), 4 genes encoding for *rsbR* paralogues, 3 sigma factor genes, 5 virulence factors and 10 genes intervening in several different metabolic pathways were extracted from *L. monocytogenes* EGD-e strain and used as query sequences. BLASTn was performed with each query sequence against all 22,340 DNA databases and then the DNA sequences were extracted for the closest match. Genes were considered absent or incomplete in a given genome assembly when either (i) the: BLASTn top hit is empty; (ii) the start or end of subject sequence is less than 20 bp from end or start of contig in which subject sequence was found; or (iii) the subject sequence is shorter than query sequence by ≥ 25 bp. Otherwise the gene was considered present and complete in genome assembly and then translated with Biopython (76) according to bacterial translate table to determine the position of stop codons and identify PMSCs (defined as codons that truncate the gene length to less than 90% the length of the gene in the reference strain EGD-e). For each gene analysed, the occurrence rate of PMSCs was calculated as a rate normalised to 100 bp to account for the different gene lengths in the analysis.

Ring formation phenotype.

Overnight cultures grown at 30°C and 2 µL were spotted onto BHI soft agar plates (0.3% w/v agar No. 2) previously dried in a laminar flow hood for 10 min. Plates were incubated at 30°C for 4 days either in constant dark or exposed to cycles of 12 h of light and dark in a blue-light array apparatus with and average intensity of 0.2 $mW.cm^{-2}$. Photographs of the grown plates were acquired using the Syngene GBox – Chemi 16 Bio Imaging System.

RNA extraction and RT-qPCR.

Overnight cultures of *L. monocytogenes* WT, Δ*sigB* and Δ*lmo0596* mutant strains were grown in BHI were adjusted to an initial OD_{600} of 0.05 in fresh BHI and allowed to grow until mid-log phase was reached (OD_{600} = 0.8) or allowed to grow overnight until stationary phase. Transcription was stopped by diluting the cultures in RNA*later*® (Sigma) in 1:5 ratio. Total RNA was extracted using RNeasy Mini Kit (Qiagen) by following the manufacturer recommendations. Cell disruption was achieved by bead-beating in FastPrep with the same parameters as mention before. Total DNA was digested with TURBO DNA-free™ (Invitrogen) digestion by following the manufacturer recommendations. RNA integrity was verified through 0.7% agarose gel electrophoresis. cDNA was synthesised with SuperScript™ IV First-Strand Synthesis System (Invitrogen) following the manufacturer recommendations and further quantified in Qubit™ (Invitrogen). RT-qPCR was performed using QuantiTect™ SYBR Green PCR Kit (Qiagen) and primer for the target genes (Table 3). Primers efficiency for the target genes 16s, *lmo2230*, sreB and *lmo0596* were determinate using purified *L. monocytogenes* genomic DNA. Samples were analysed on LightCycler® 480 System (Roche) with the following parameters, 95°C for 15 min, 45 cycles of 15 s at 95°C, 15 s at 53°C and 30 s at 72°C, a melting curve was drawn for 5 s at 95°C, 1 min at 55°C followed by increases of $0.11°C.s^{-1}$ until 95°C, and a cooling for 30 s at 40°C. Cycle quantification values were calculated by the software LightCycler® 480 Software version 1.5.1 (Roche) and the Pfaffl relative expression formula (77, 78). The expression of the 16s rDNA was used as reference gene. Three biological replicates, each in technical duplicates were performed. Results are expressed in Log_2 relative expression ratio normalized against the WT strain.

Statistical analysis.

Student's *t*-test analysis was performed on GraphPad Prism 8.

Acknowledgements

738 This project has received funding from the European Union's Horizon 2020 research
739 and innovation programme under the Marie Skłodowska-Curie grant agreement No.
740 721456. Jialun Wu was funded by the Department of Agriculture, Food and the Marine
741 (17/F/244).
742 The authors wish to acknowledge Nicholas Waters for the help in scripting.
743
744

745 **References**

746 1. Mylonakis E, Paliou M, Hohmann EL, Calderwood SB, Wing EJ. 2002. Listeriosis
747 during pregnancy: a case series and review of 222 cases. Medicine 81:260-269.
748 2. Farber J, Peterkin P. 1991. Listeria monocytogenes, a food-borne pathogen.
749 Microbiology and Molecular Biology Reviews 55:476-511.
750 3. Barbuddhe SB, Chakraborty T. 2009. Listeria as an enteroinvasive
751 gastrointestinal pathogen, p 173-195, Molecular mechanisms of bacterial
752 infection via the gut. Springer.
753 4. Gandhi M, Chikindas ML. 2007. Listeria: a foodborne pathogen that knows how
754 to survive. International journal of food microbiology 113:1-15.
755 5. Jensen VB, Harty JT, Jones BD. 1998. Interactions of the Invasive
756 PathogensSalmonella typhimurium, Listeria monocytogenes, and Shigella
757 flexneri with M Cells and Murine Peyer's Patches. Infection and immunity
758 66:3758-3766.
759 6. Liu Y, Orsi RH, Boor KJ, Wiedmann M, Guariglia-Oropeza V. 2017. Home alone:
760 elimination of all but one alternative sigma factor in Listeria monocytogenes
761 allows prediction of new roles for σB. Frontiers in microbiology 8:1910.
762 7. Chaturongakul S, Raengpradub S, Palmer ME, Bergholz TM, Orsi RH, Hu Y,
763 Ollinger J, Wiedmann M, Boor KJ. 2011. Transcriptomic and phenotypic analyses
764 identify coregulated, overlapping regulons among PrfA, CtsR, HrcA, and the
765 alternative sigma factors σB, σC, σH, and σL in Listeria monocytogenes. Applied
766 and environmental microbiology 77:187-200.
767 8. Sleator RD, Watson D, Hill C, Gahan CG. 2009. The interaction between Listeria
768 monocytogenes and the host gastrointestinal tract. Microbiology 155:2463-2475.
769 9. Kim H, Marquis H, Boor KJ. 2005. σB contributes to Listeria monocytogenes
770 invasion by controlling expression of inlA and inlB. Microbiology (Reading,
771 England) 151:3215.
772 10. Wise AA, Price CW. 1995. Four additional genes in the sigB operon of Bacillus
773 subtilis that control activity of the general stress factor sigma B in response to
774 environmental signals. Journal of bacteriology 177:123-133.
775 11. Toledo-Arana A, Dussurget O, Nikitas G, Sesto N, Guet-Revillet H, Balestrino D,
776 Loh E, Gripenland J, Tiensuu T, Vaitkevicius K. 2009. The Listeria transcriptional
777 landscape from saprophytism to virulence. Nature 459:950.

12. Ferreira A, Gray M, Wiedmann M, Boor KJ. 2004. Comparative genomic analysis of the sigB operon in Listeria monocytogenes and in other Gram-positive bacteria. Current microbiology 48:39-46.
13. Boylan SA, Rutherford A, Thomas SM, Price CW. 1992. Activation of Bacillus subtilis transcription factor sigma B by a regulatory pathway responsive to stationary-phase signals. Journal of Bacteriology 174:3695-3706.
14. Benson AK, Haldenwang WG. 1992. Characterization of a regulatory network that controls sigma B expression in Bacillus subtilis. Journal of Bacteriology 174:749-757.
15. Marles-Wright J, Lewis RJ. 2010. The stressosome: molecular architecture of a signalling hub. Portland Press Limited.
16. Pané-Farré J, Quin MB, Lewis RJ, Marles-Wright J. 2017. Structure and function of the stressosome signalling hub, p 1-41, Macromolecular Protein Complexes. Springer.
17. Impens F, Rolhion N, Radoshevich L, Bécavin C, Duval M, Mellin J, del Portillo FG, Pucciarelli MG, Williams AH, Cossart P. 2017. N-terminomics identifies Prli42 as a membrane miniprotein conserved in Firmicutes and critical for stressosome activation in Listeria monocytogenes. Nature microbiology 2:17005.
18. Martinez L, Reeves A, Haldenwang W. 2010. Stressosomes formed in Bacillus subtilis from the RsbR protein of Listeria monocytogenes allow σB activation following exposure to either physical or nutritional stress. Journal of bacteriology 192:6279-6286.
19. Ondrusch N, Kreft J. 2011. Blue and red light modulates SigB-dependent gene transcription, swimming motility and invasiveness in Listeria monocytogenes. PloS one 6:e16151.
20. Delumeau O, Chen C-C, Murray JW, Yudkin MD, Lewis RJ. 2006. High-molecular-weight complexes of RsbR and paralogues in the environmental signaling pathway of Bacillus subtilis. Journal of bacteriology 188:7885-7892.
21. Gaidenko TA, Yang X, Lee YM, Price CW. 1999. Threonine phosphorylation of modulator protein RsbR governs its ability to regulate a serine kinase in the environmental stress signaling pathway of Bacillus subtilis 1. Journal of molecular biology 288:29-39.
22. Kim T-J, Gaidenko TA, Price CW. 2004. A multicomponent protein complex mediates environmental stress signaling in Bacillus subtilis. Journal of molecular biology 341:135-150.
23. Yang X, Kang CM, Brody MS, Price CW. 1996. Opposing pairs of serine protein kinases and phosphatases transmit signals of environmental stress to activate a bacterial transcription factor. Genes & development 10:2265-2275.
24. Utratna M, Cosgrave E, Baustian C, Ceredig R, O'Byrne C. 2012. Development and optimization of an EGFP-based reporter for measuring the general stress response in Listeria monocytogenes. Bioengineered 3:93-103.
25. Kang CM, Vijay K, Price CW. 1998. Serine kinase activity of a Bacillus subtilis switch protein is required to transduce environmental stress signals but not to activate its target PP2C phosphatase. Molecular microbiology 30:189-196.

26. Kim T-J, Gaidenko TA, Price CW. 2004. In vivo phosphorylation of partner switching regulators correlates with stress transmission in the environmental signaling pathway of Bacillus subtilis. Journal of bacteriology 186:6124-6132.
27. Shin J-H, Brody MS, Price CW. 2010. Physical and antibiotic stresses require activation of the RsbU phosphatase to induce the general stress response in Listeria monocytogenes. Microbiology 156:2660.
28. Tran V, Geraci K, Midili G, Satterwhite W, Wright R, Bonilla CY. 2018. Resilience to oxidative and nitrosative stress is mediated by the stressosome, RsbP and SigB in Bacillus subtilis. bioRxiv:460303.
29. Chaturongakul S, Boor KJ. 2004. RsbT and RsbV contribute to σB-dependent survival under environmental, energy, and intracellular stress conditions in Listeria monocytogenes. Applied and environmental microbiology 70:5349-5356.
30. Brøndsted L, Kallipolitis BH, Ingmer H, Knöchel S. 2003. kdpE and a putative RsbQ homologue contribute to growth of Listeria monocytogenes at high osmolarity and low temperature. FEMS microbiology letters 219:233-239.
31. O'Donoghue B. 2016. A molecular genetic investigation into stress sensing in the food-borne pathogen Listeria Monocytogenes: roles for RsbR and its paralogues, Doctoral Thesis. National University of Ireland, Galway, Ireland. URL: http://hdl.handle.net/10379/6310.
32. Tiensuu T, Andersson C, Rydén P, Johansson J. 2013. Cycles of light and dark co-ordinate reversible colony differentiation in Listeria monocytogenes. Molecular microbiology 87:909-924.
33. Hauf S, Herrmann J, Miethke M, Gibhardt J, Commichau FM, Müller R, Fuchs S, Halbedel S. 2019. Aurantimycin resistance genes contribute to survival of Listeria monocytogenes during life in the environment. Molecular microbiology.
34. Hingston P, Chen J, Dhillon BK, Laing C, Bertelli C, Gannon V, Tasara T, Allen K, Brinkman FS, Truelstrup Hansen L. 2017. Genotypes associated with Listeria monocytogenes isolates displaying impaired or enhanced tolerances to cold, salt, acid, or desiccation stress. Frontiers in microbiology 8:369.
35. Asakura H, Kawamoto K, Okada Y, Kasuga F, Makino S-i, Yamamoto S, Igimi S. 2012. Intrahost passage alters SigB-dependent acid resistance and host cell-associated kinetics of Listeria monocytogenes. Infection, Genetics and Evolution 12:94-101.
36. Quereda JJ, Pucciarelli MG, Botello-Morte L, Calvo E, Carvalho F, Bouchier C, Vieira A, Mariscotti JF, Chakraborty T, Cossart P. 2013. Occurrence of mutations impairing sigma factor B (SigB) function upon inactivation of Listeria monocytogenes genes encoding surface proteins. Microbiology 159:1328-1339.
37. Loh E, Dussurget O, Gripenland J, Vaitkevicius K, Tiensuu T, Mandin P, Repoila F, Buchrieser C, Cossart P, Johansson J. 2009. A trans-acting riboswitch controls expression of the virulence regulator PrfA in Listeria monocytogenes. Cell 139:770-779.
38. Rauch M, Luo Q, Müller-Altrock S, Goebel W. 2005. SigB-dependent in vitro transcription of prfA and some newly identified genes of Listeria monocytogenes whose expression is affected by PrfA in vivo. Journal of bacteriology 187:800-804.

39. Utratna M, Shaw I, Starr E, O'Byrne CP. 2011. Rapid, transient, and proportional activation of σB in response to osmotic stress in Listeria monocytogenes. Appl Environ Microbiol 77:7841-7845.
40. Utratna M, Cosgrave E, Baustian C, Ceredig RH, O'Byrne CP. 2014. Effects of growth phase and temperature on activity within a Listeria monocytogenes population: evidence for RsbV-independent activation of at refrigeration temperatures. BioMed research international 2014.
41. Zhang Z, Meng Q, Qiao J, Yang L, Cai X, Wang G, Chen C, Zhang L. 2013. RsbV of Listeria monocytogenes contributes to regulation of environmental stress and virulence. Archives of microbiology 195:113-120.
42. Cao M, Bitar AP, Marquis H. 2007. A mariner-based transposition system for Listeria monocytogenes. Appl Environ Microbiol 73:2758-2761.
43. Chen CC, Lewis RJ, Harris R, Yudkin MD, Delumeau O. 2003. A supramolecular complex in the environmental stress signalling pathway of Bacillus subtilis. Molecular microbiology 49:1657-1669.
44. Eymann C, Schulz S, Gronau K, Becher D, Hecker M, Price CW. 2011. In vivo phosphorylation patterns of key stressosome proteins define a second feedback loop that limits activation of Bacillus subtilis σB. Molecular microbiology 80:798-810.
45. Fu Z, Tamber S, Memmi G, Donegan NP, Cheung AL. 2009. Overexpression of MazFsa in Staphylococcus aureus induces bacteriostasis by selectively targeting mRNAs for cleavage. Journal of bacteriology 191:2051-2059.
46. Schuster CF, Mechler L, Nolle N, Krismer B, Zelder M-E, Götz F, Bertram R. 2015. The MazEF toxin-antitoxin system alters the β-lactam susceptibility of Staphylococcus aureus. PLoS One 10:e0126118.
47. Curtis TD, Takeuchi I, Gram L, Knudsen GM. 2017. The Influence of the Toxin/Antitoxin mazEF on Growth and Survival of Listeria monocytogenes under Stress. Toxins 9:31.
48. Orsi R, Ripoll D, Yeung M, Nightingale K, Wiedmann M. 2007. Recombination and positive selection contribute to evolution of Listeria monocytogenes inlA. Microbiology 153:2666-2678.
49. Dorey A, Marinho C, Piveteau P, O'Byrne C. 2019. Role and regulation of the stress activated sigma factor sigma B (σB) in the saprophytic and host-associated life stages of Listeria monocytogenes. Advances in applied microbiology 106:1-48.
50. Tiensuu T, Guerreiro DN, Oliveira AH, O'Byrne C, Johansson J. 2019. Flick of a switch: regulatory mechanisms allowing Listeria monocytogenes to transition from a saprophyte to a killer. Microbiology 165:819-833.
51. Marles-Wright J, Lewis RJ. 2008. The Bacillus subtilis stressosome: A signal integration and transduction hub. Communicative & integrative biology 1:182-184.
52. Voelker U, Voelker A, Haldenwang WG. 1996. Reactivation of the Bacillus subtilis anti-sigma B antagonist, RsbV, by stress-or starvation-induced phosphatase activities. Journal of bacteriology 178:5456-5463.
53. Holtmann G, Brigulla M, Steil L, Schütz A, Barnekow K, Völker U, Bremer E. 2004. RsbV-independent induction of the SigB-dependent general stress regulon

of Bacillus subtilis during growth at high temperature. Journal of bacteriology 186:6150-6158.
54. Brigulla M, Hoffmann T, Krisp A, Völker A, Bremer E, Völker U. 2003. Chill induction of the SigB-dependent general stress response in Bacillus subtilis and its contribution to low-temperature adaptation. Journal of bacteriology 185:4305-4314.
55. Hsu C-Y, Cairns L, Hobley L, Abbott J, O'Byrne C, Stanley-Wall NR. 2020. Genomic differences between Listeria monocytogenes EGDe isolates reveals crucial roles for SigB and wall rhamnosylation in biofilm formation. Journal of Bacteriology.
56. Arnaud M, Chastanet A, Débarbouillé M. 2004. New vector for efficient allelic replacement in naturally nontransformable, low-GC-content, gram-positive bacteria. Appl Environ Microbiol 70:6887-6891.
57. Abram F, Starr E, Karatzas K-AG, Matlawska-Wasowska K, Boyd A, Wiedmann M, Boor K, Connally D, O'Byrne C. 2008. Identification of components of the sigma B regulon in Listeria monocytogenes that contribute to acid and salt tolerance. Applied and environmental microbiology 74:6848-6858.
58. Schweder T, Kolyschkow A, Völker U, Hecker M. 1999. Analysis of the expression and function of the σB-dependent general stress regulon of Bacillus subtilis during slow growth. Archives of microbiology 171:439-443.
59. O'Donoghue B, NicAogáin K, Bennett C, Conneely A, Tiensuu T, Johansson J, O'Byrne C. 2016. Blue-light inhibition of Listeria monocytogenes growth is mediated by reactive oxygen species and is influenced by σB and the blue-light sensor Lmo0799. Applied and environmental microbiology 82:4017-4027.
60. Finkel SE. 2006. Long-term survival during stationary phase: evolution and the GASP phenotype. Nature Reviews Microbiology 4:113.
61. Zambrano MM, Kolter R. 1996. GASPing for life in stationary phase. Cell 86:181-184.
62. Liu B, Eydallin G, Maharjan RP, Feng L, Wang L, Ferenci T. 2017. Natural Escherichia coli isolates rapidly acquire genetic changes upon laboratory domestication. Microbiology 163:22-30.
63. Maharjan R, Nilsson S, Sung J, Haynes K, Beardmore RE, Hurst LD, Ferenci T, Gudelj I. 2013. The form of a trade-off determines the response to competition. Ecology letters 16:1267-1276.
64. Gudelj I, Weitz JS, Ferenci T, Claire Horner-Devine M, Marx CJ, Meyer JR, Forde SE. 2010. An integrative approach to understanding microbial diversity: from intracellular mechanisms to community structure. Ecology letters 13:1073-1084.
65. Farewell A, Kvint K, Nyström T. 1998. Negative regulation by RpoS: a case of sigma factor competition. Molecular microbiology 29:1039-1051.
66. Notley-McRobb L, King T, Ferenci T. 2002. rpoS mutations and loss of general stress resistance in Escherichia coli populations as a consequence of conflict between competing stress responses. Journal of bacteriology 184:806-811.
67. Nyström T. 2004. MicroReview: Growth versus maintenance: a trade-off dictated by RNA polymerase availability and sigma factor competition? Molecular microbiology 54:855-862.

68. Marinho CM, Dos Santos PT, Kallipolitis BH, Johansson J, Ignatov D, Guerreiro DN, Piveteau P, O'Byrne CP. 2019. The σB-dependent regulatory sRNA Rli47 represses isoleucine biosynthesis in Listeria monocytogenes through a direct interaction with the ilvA transcript. RNA biology:1-15.
69. Monk IR, Gahan CG, Hill C. 2008. Tools for functional postgenomic analysis of listeria monocytogenes. Appl Environ Microbiol 74:3921-34.
70. Deatherage DE, Barrick JE. 2014. Identification of mutations in laboratory-evolved microbes from next-generation sequencing data using breseq, p 165-188, Engineering and analyzing multicellular systems. Springer.
71. Darling AC, Mau B, Blattner FR, Perna NT. 2004. Mauve: multiple alignment of conserved genomic sequence with rearrangements. Genome research 14:1394-1403.
72. Collins TJ. 2007. ImageJ for microscopy. BioTechniques 43:S25-S30.
73. Hamilton N. 2009. Quantification and its applications in fluorescent microscopy imaging. Traffic 10:951-961.
74. Selinummi J, Seppälä J, Yli-Harja O, Puhakka JA. 2005. Software for quantification of labeled bacteria from digital microscope images by automated image analysis. Biotechniques 39:859-863.
75. Salcedo C, Arreaza L, Alcala B, De La Fuente L, Vazquez J. 2003. Development of a multilocus sequence typing method for analysis of Listeria monocytogenes clones. Journal of clinical microbiology 41:757-762.
76. Cock PJ, Antao T, Chang JT, Chapman BA, Cox CJ, Dalke A, Friedberg I, Hamelryck T, Kauff F, Wilczynski B. 2009. Biopython: freely available Python tools for computational molecular biology and bioinformatics. Bioinformatics 25:1422-1423.
77. Pfaffl MW. 2001. A new mathematical model for relative quantification in real-time RT–PCR. Nucleic acids research 29:e45-e45.
78. Pfaffl M, Georgieva TM, Georgiev IP, Ontsouka E, Hageleit M, Blum J. 2002. Real-time RT-PCR quantification of insulin-like growth factor (IGF)-1, IGF-1 receptor, IGF-2, IGF-2 receptor, insulin receptor, growth hormone receptor, IGF-binding proteins 1, 2 and 3 in the bovine species. Domestic animal endocrinology 22:91-102.
79. den Dunnen JT, Dalgleish R, Maglott DR, Hart RK, Greenblatt MS, McGowan-Jordan J, Roux AF, Smith T, Antonarakis SE, Taschner PE. 2016. HGVS recommendations for the description of sequence variants: 2016 update. Human mutation 37:564-569.

997 **Figures captions**

998

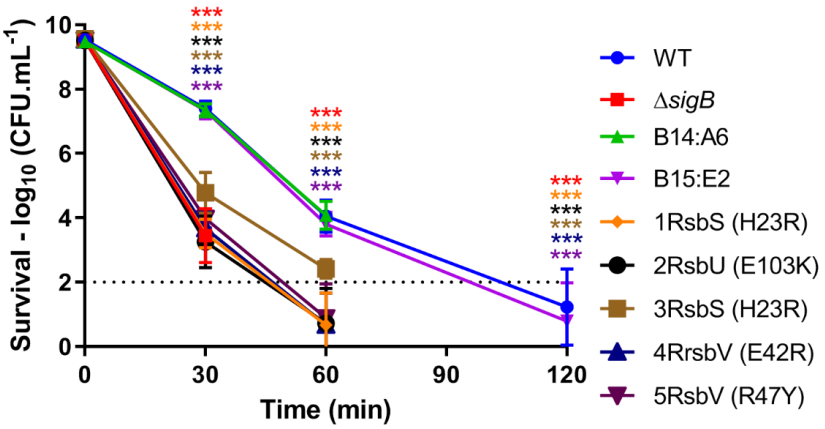

FIG 1 "Ringless" transposon mutant strains have acid sensitive phenotypes. Stationary phase cultures grown in BHI at 37°C before being challenged in acidified BHI (pH 2.5) at 37°C. At 0, 30, 50 and 120 min, samples were taken for viable counts measurement. Dotted line represents the detection threshold. Each marker represents the measurement average of three independent biological replicates performed, with the respective standard deviation. Statistical analysis was performed using a paired Student *t*-test (*** = *p*-value < 0.001).

999

1000

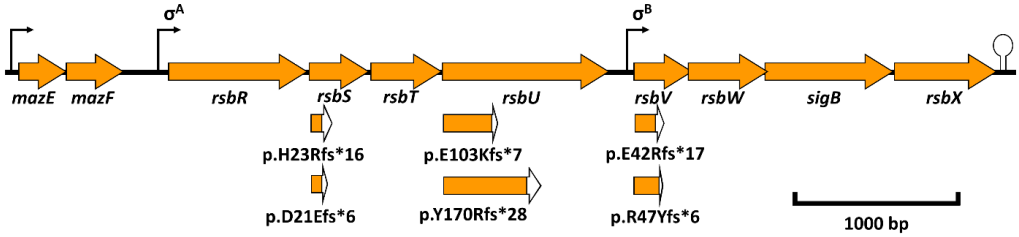

FIG 2 Locations of the frameshift mutations in the *sigB* operon. Layout of the *sigB* operon with the respective promoter regions and terminator. Each arrow representing the ORF of *mazE*, *mazF*, *rsbR*, *rsbS*, *rsbT*, *rsbU*, *rsbV*, *rsbW*, *sigB* and *rsbX* with the respective location of the identified mutations. White sections of the ORF represent the alternate reading frame produced by the frameshift mutations in *rsbS*, *rsbU* and *rsbV* until a PMSC is encoded.

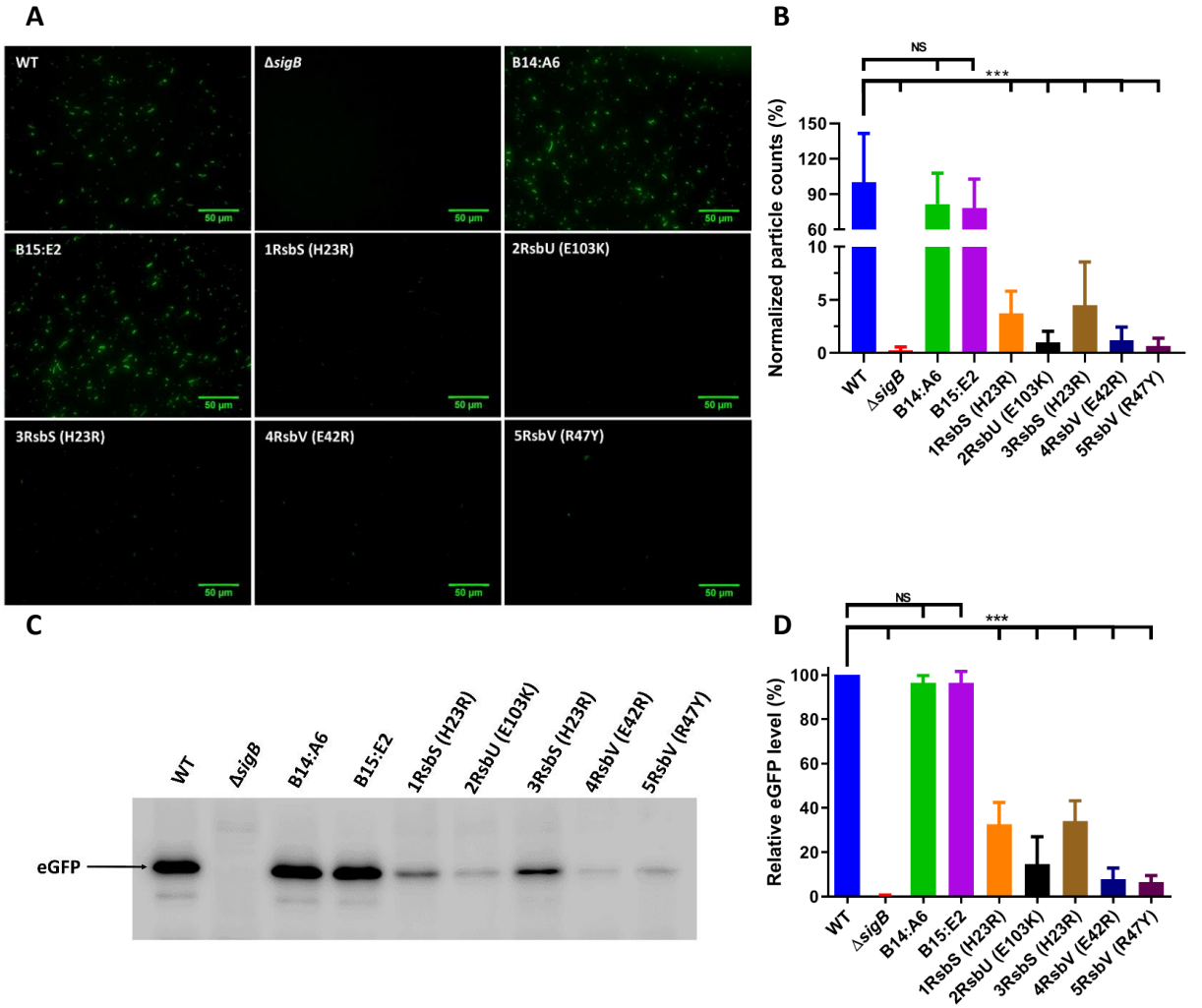

FIG 3 Transposon mutant strains carrying *sigB* operon mutations all have decreased σ^B activity. Stationary phase cultures grown at 37°C of WT, Δ*sigB* and transposon mutant strains transformed with pKSV7-P$_{lmo2230}$::*egfp*. Measurements of fluorescence were made through (A) images obtained by fluorescence microscopy (B) Particle quantification from fluorescence microscopy images. A total of 15 images were taken across three biological replicates. Particle counts were normalized against the WT strain and converted to percentage. (C) western-blot using anti-GFP antibodies, arrow shows eGFP protein with a size of 27 kDa. (D) Percentage of eGFP quantification normalized against the WT obtained from western-blot images. Data generated from three independent biological replicates. Statistical analysis performed through a paired Student *t*-test (* = *p*-value < 0.05; ** = *p*-value < 0.01; *** = *p*-value < 0.001; NS – non-significant).

1001

1002

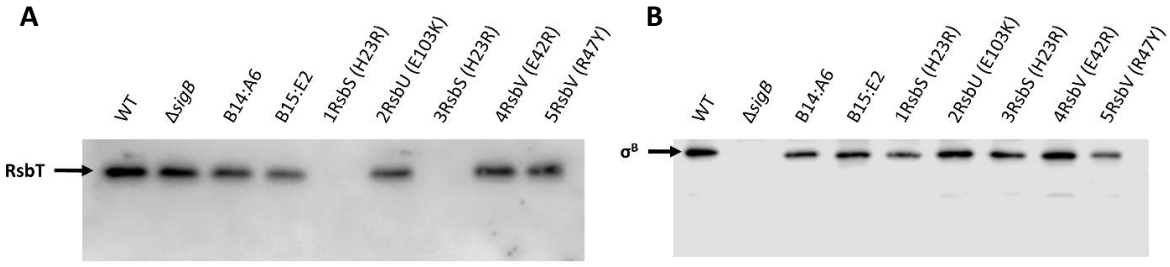

FIG 4 Frameshift mutations in *rsbS* produce a polar effect resulting in the inhibition of RsbT translation. Western-blot images obtained from total protein extractions of stationary phase WT, Δ*sigB*, and transposon mutant strains grown at 37°C. Western-blots were probed with rabbit polyclonal (A) anti-RsbT and (B) anti-σ^B antibodies. Arrows point to the respective proteins, RsbT with a predicted size of 14.7 kDa and σ^B with 29.5 kDa.

1003

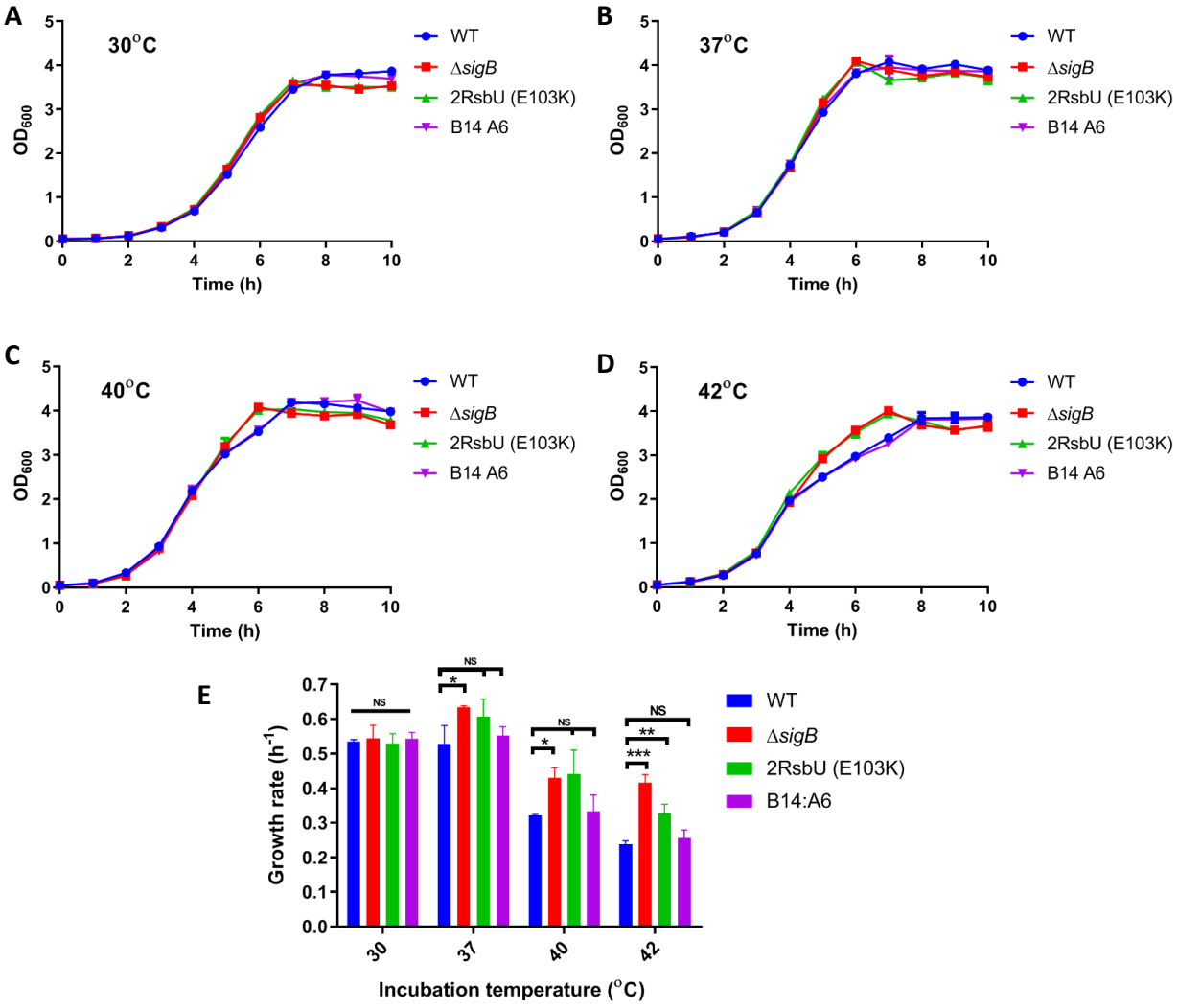

FIG 5 Loss of σ^B activity associated with increased growth rate at elevated temperatures. Measurements of OD_{600} of WT, Δ*sigB*, 2RsbU (E103K) and B14:A6 were performed every hour for 12 hours in BHI at (A) 30°C, (B) 37°C, (C) 40°C and (D) 42°C. (E) Growth rates in hours were calculated by using Log_{10} (OD_{600}) of the transition period from data points between 4 and 5 hours (for 37°C, 40°C and 42°C) and 5 and 6 (30°C). Data generated for three biological replicates. Statistical analysis was performed using a paired Student *t*-test (* = *p*-value < 0.05; ** = *p*-value < 0.01; *** = *p*-value < 0.001; NS – non-significant).

1004

1005

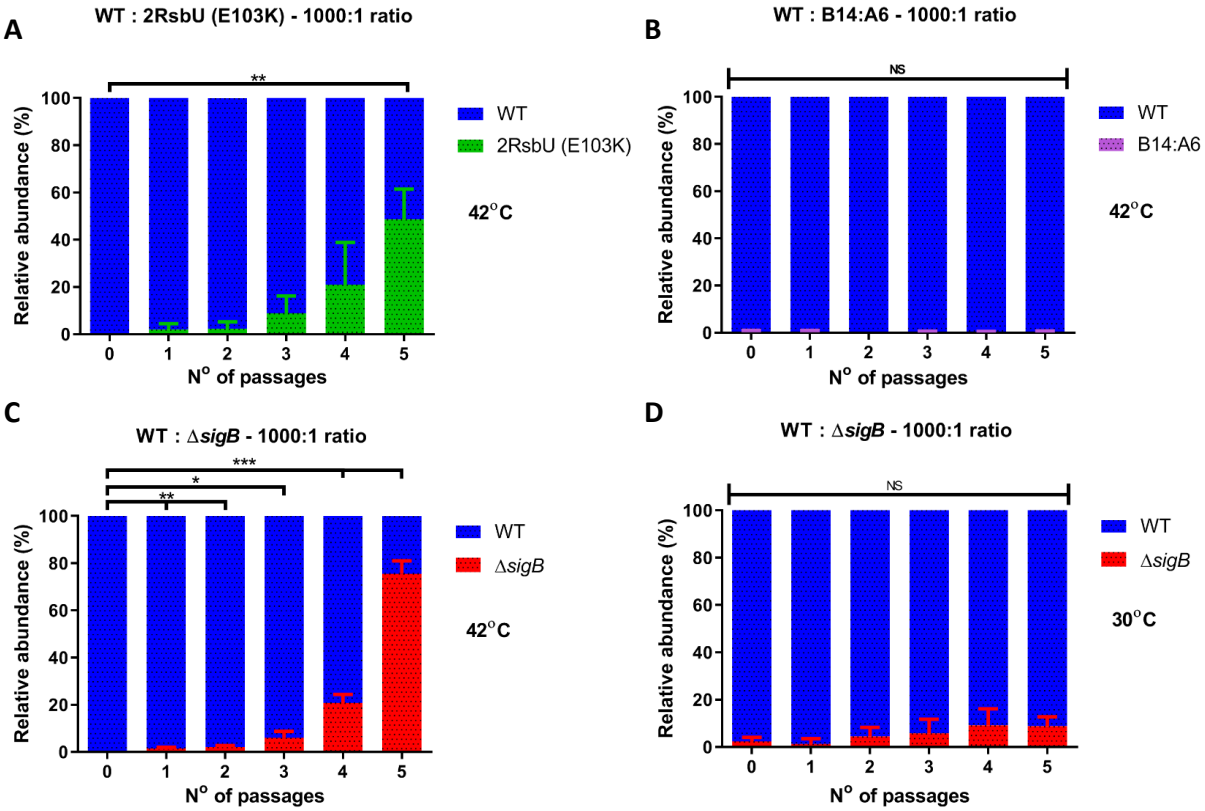

FIG 6 Loss of σ^B activity is associated with a competitive advantage at 42˚C. Cultures mixed in ratios of 1000:1 of (A) WT with 2RsbU (E103K), (B) WT with B14:A6, (C) WT with Δ*sigB* incubated at 42°C and (D) WT with Δ*sigB* incubated at 30°C. Passages were made every 24 hours for 5 days. WT and transposon mutant strains were distinguished by erythromycin resistance. WT and Δ*sigB* mutant strains were distinguished by colony coloration. Results are depicted in relative abundance of $CFU.mL^{-1}$. Data generated for three independent biological replicates. Statistical analysis was performed using a paired Student *t*-test (* = *p*-value < 0.05; ** = *p*-value < 0.01; *** = *p*-value < 0.001; NS – non-significant).

1006

1007

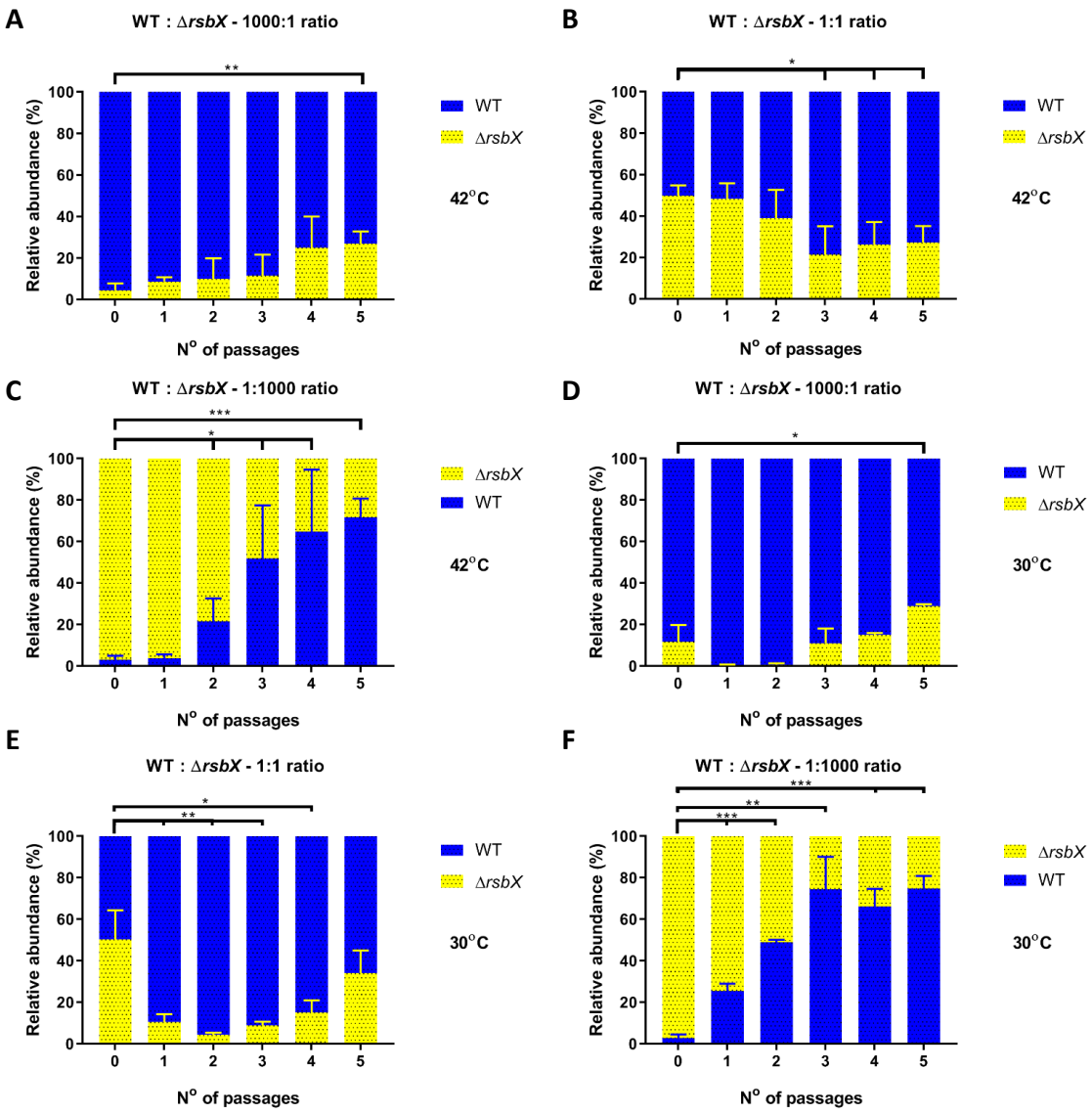

FIG 7 Competitive advantage of WT strain when challenged against Δ*rsbX* mutant strain at both 30°C and 42°C. Competition experiments of mixed cultures of WT and Δ*rsbX* mutant strains performed at 42°C and 30°C, showing the relative abundance in percentage of CFU.mL^{-1}. Cultures incubated at 42°C were mixed in ratios of (A) 1000:1 (B) 1:1, (C) 1:1000 of WT:Δ*rsbX*, respectively. The same ratios were mixed and incubated at 30°C in (D), (E) and (F). Passages were made every 24 hours for 5 days. Statistical analysis performed through a paired Student *t*-test (* = *p*-value < 0.05; ** = *p*-value < 0.01; *** = *p*-value < 0.001).

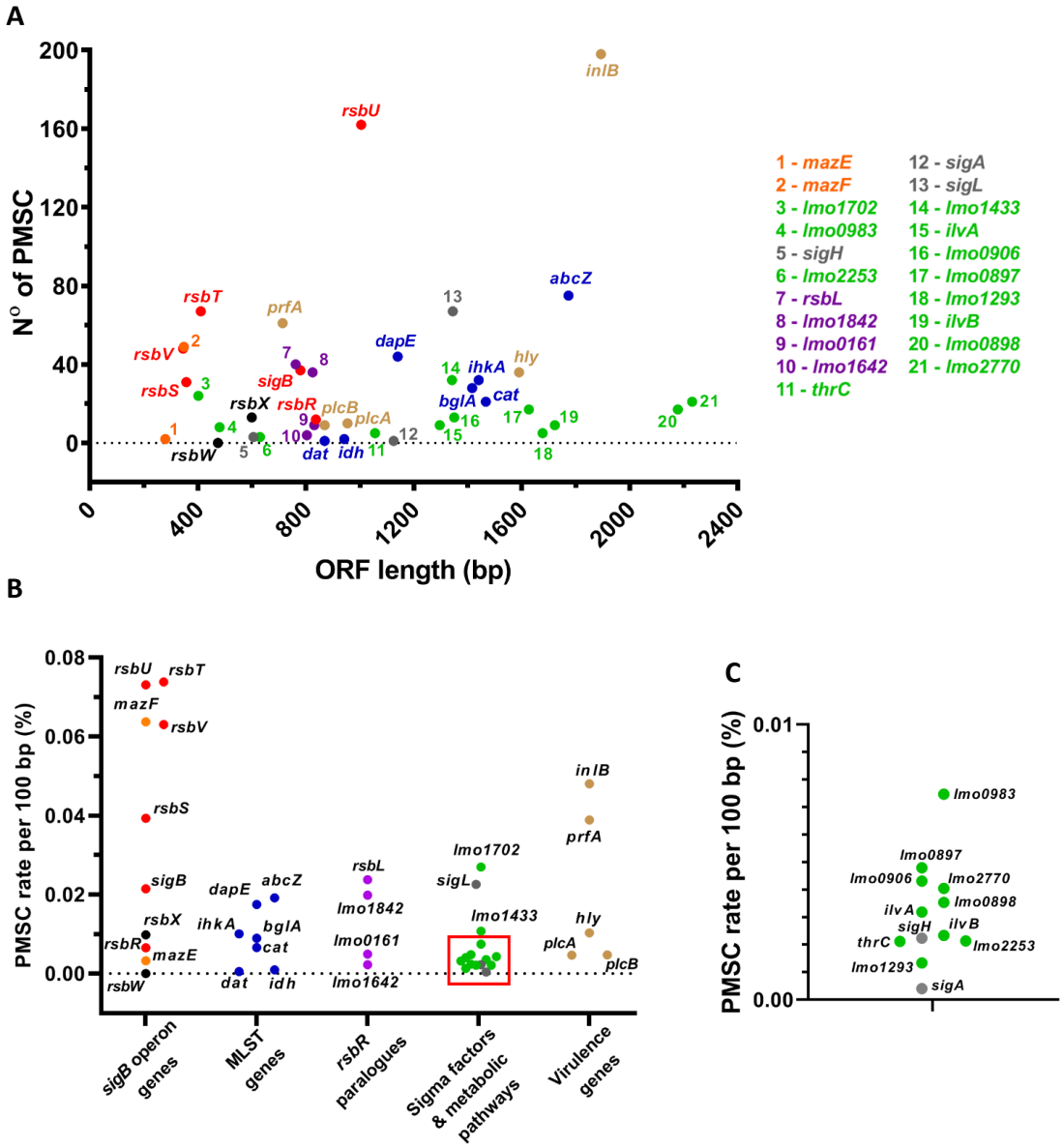

FIG 8 Occurrence of PMSCs is elevated in genes encoding positive effectors of σ^B activity. Results of the PMSC mutations retrieved from the *in silico* analysis of the 22,340 genomes *L. monocytogenes* strains available. (A) The total number of identified PMSC by the ORF length in base pairs and (B) PMSC rate normalized by 100 bp of the ORF length, displaying genes compromising the *sigB* operon and characterized as putative positive regulator of σ^B activity are displayed (red), the putative σ^B negative regulator *rsbX* and *rsbW* (black) and *mazEF* (orange) genes. MLST genes are displayed (blue), *rsbR* paralogues (purple). Housekeeping gene *sigA* and the sigma factors *sigL* and *sigH* (grey). Two genes downstream of the *sigB* operon, *lmo0897* and *lmo0898* and genes encoding for metabolic pathways of glutathione (*lmo1702, lmo0983, lmo1433, lmo0906* and *lmo2770*), glycerol (*lmo1293*), threonine (*thrC*), isoleucine (*ilvA* and *ilvB*) and glucose (*lmo2253*) (green) and *prfA*, *inlB*, *hly*, *plcA* and *plcB* (brown), respectively. The area indicated by the Red square area is expanded in (C).

1010 **Table 1 List of strains and plasmids used for this study.**

Strains and plasmids[a]	Transposon[b]	Ring formation[e]	Source
pKSV7-P*lmo2230*::*egfp*	NA	NA	(24)
pMAD	NA	NA	(56)
pMAD::Δ*sigB*	NA	NA	(68)
pMAD::Δ*rsbX*	NA	NA	This study
pEX-K168::Δlmo0596	NA	NA	Eurofins genomic
pMAD::Δ*lmo0596*	NA	NA	This study
Escherichia coli One Shot™ TOP10	NA	NA	Invitrogen
L. monocytogenes EGD-e WT	-	+	K. Boor
L. monocytogenes EGD-e Δ*sigB*	-	-	This study
L. monocytogenes EGD-e Δ*rsbX*	-	NA	This study
L. monocytogenes EGD-e Δ*lmo0596*	-	+	This study
L. monocytogenes EGD-e Δ*sreB*	-	+	(37)
L. monocytogenes EGD-e A4:E8[c] (1RsbS (H23R))[d]	+	-	(32)
L. monocytogenes EGD-e A4:D7[c]	+	-	(32)
L. monocytogenes EGD-e A1:D10[c]	+	-	(32)
L. monocytogenes EGD-e A4:B1[c]	+	-	(32)
L. monocytogenes EGD-e A3:G10[c]	+	-	(32)
L. monocytogenes EGD-e C10:A8[c];(2RsbU (E103K))[d]	+	-	(32)
L. monocytogenes EGD-e C14:C12[c]; (3RsbS (H23R))[d]	+	-	(32)
L. monocytogenes EGD-e C12:F3[c]	+	-	(32)
L. monocytogenes EGD-e C9:C1[c]	+	-	(32)
L. monocytogenes EGD-e D9:B6[c]; (4RsbV (E42R))[d]	+	-	(32)
L. monocytogenes EGD-e D2:C10[c]; (5RsbV (R47Y))[d]	+	-	(32)
L. monocytogenes EGD-e B14:A6[c]	+	+	(32)
L. monocytogenes EGD-e B15:E2[c]	+	+	(32)

eGFP reporter strains	Source
L. monocytogenes EGD-e WT/pKSV7-P*lmo2230*::*egfp*	(24)
L. monocytogenes EGD-e Δ*sigB*/pKSV7-P*lmo2230*::*egfp*	This study
L. monocytogenes EGD-e A4:E8/pKSV7-P*lmo2230*::*egfp*	This study
L. monocytogenes EGD-e C10:A8/pKSV7-P*lmo2230*::*egfp*	This study
L. monocytogenes EGD-e C14:C12/pKSV7-P*lmo2230*::*egfp*	This study
L. monocytogenes EGD-e D9:B6/pKSV7-P*lmo2230*::*egfp*	This study
L. monocytogenes EGD-e D2:C10/pKSV7-P*lmo2230*::*egfp*	This study
L. monocytogenes EGD-e B14:A6/pKSV7-P*lmo2230*::*egfp*	This study

[a] see Table 2 for full genotype description.
[b] presence/absence of chromosomal *mariner*-based transposon insertion.
[c] nomenclature consistent with Tiensuu et al. (32).
[d] transposon mutant strain new designation.
[e] Ring formation on soft agar plates in response to cycles of light/dark (ring formation requires σ^B)
NA – not applicable

1011

1012

1013 **Table 2 WGS results for *L. monocytogenes* EGD-e transposon mutant strains.**

Strain code (32)	Transposon location (32)	Transposon location (by WGS)	SNP location in *sigB* operon[a]	Frameshift result[f]	New strain name
A4:E8	*lmo0040*	*lmo0770*[c]	IN(*rsbS*)*67* (+GATC)	p.H23Rfs*16	1RsbS (H23R)
A4:D7	*lmo0101/lmo0102*[b]	[e]	IN(*rsbS*)*67* (+GATC)	p.H23Rfs*16	NA
A1:D10	*lmo0842*	[e]	IN(*rsbS*)*67* (+GATC)	p.H23Rfs*16	NA
A4:B1	*lmo2682*	[e]	IN(*rsbS*)*67* (+GATC)	p.H23Rfs*16	NA
A3:G10	*lmo2777*	[e]	IN(*rsbS*)*67* (+GATC)	p.H23Rfs*16	NA
C10:A8	*lmo0124*	*lmo0125*[c]	Δ(*rsbU*)*306* (-G)	p.E103Kfs*7	2RsbU (E103K)
C14:C12	*lmo0595/lmo0596*[b]	[e]	IN(*rsbS*)*67* (+GATC)	p.H23Rfs*16	3RsbS (H23R)
C12:F3	*lmo0774*	[e]	Δ(*rsbU*)*506* (-AT)	p.Y170Rfs*28	NA
C9:C1	*lmo1736*	[e]	Δ(*rsbS*)*6* (-T)	p.D21Efs*6	NA
D9:B6	*lmo0101*	*lmo0101/lmo0102*[b,c,d]	IN(*rsbV*)*136* (+TGTAC)	p.R47Yfs*6	4RsbV (E42R)
D2:C10	*lmo2668*	[e]	IN(*rsbV*)*120* (+A)	p.E42Rfs*17	5RsbV (R47Y)
B14:A6	[g]	*lmo1671*	None	NA	NA
B15:E2	[g]	*lmo2287*	None	NA	NA

[a] SNP position in *L. monocytogenes* chromosome identified by WGS.

[b] Transposon insertion located in intergenic region.

[c] Different transposon position than initially reported.

[d] Not in the same position as A4:D7.

[e] Same position as reported (32).

[f] Nomenclature adapted from Human Genome Variations Society (79). For example, in "p.H23Rfs*16", p.H23R refers to the first encoded residue affected in the new protein, resulting in a histidine to arginine substitution at the codon 23, while fs*16 refers to the number of codons in the new reading frame that would be translated prior to encountering a stop codon.

[g] Not previously analysed through WGS (32).

NA – not applicable.

1014

1015 **Table 3 List primers used for this study.**

1016

Primer sequence (5' to 3')	Target
GCCTTGTCGCCATCTTTG	*egfp-lmo2230*-F integration
1017 GGCCGTTTACATCTCCATC	*egfp-lmo2230*-R integration
ATAACGGCACAAGCTTCG	*sigB*-flank_F
TTATGGCGTCAACAGTCG	*sigB*-flank_R
GGAGTAAATGAACAAGGCAG	*rsbX*-flank_F
CGCTAGTTTAAAAGGTGTTATGG	*rsbX*-flank_R
CGGTCGACGTAGAGTCCATCGCCCGAA	*rsbX*-A
TTACTCCACTTCCTCATTCTGCAAC	*rsbX*-B
AATGAGGAAGTGGAGTAACCATAACACC	*rsbX*-C
CGAGATCTATCATTCCGGCAACAAGTAAATCTTGG	*rsbX*-D
CTAGCTAATGTTACGTTACA	pMAD-U
GCGAGAAGAATCATAATGGG	pMAD-L
GAAAATAAATTCCGGTTGCTAAGGC	*lmo0596*-A
AATCGAGTCGGATGGTTCTTGTT	*lmo0596*-B
CCACTCCTCTTTGATATGTATTTAT	*lmo0596*-flank_F
GGCAGATGAATGCACTTATG	*lmo0596*-flank_R
Primer sequence for RT-qPCR (5' to 3')	**Target**
TGGGGAGCAAACAGGATTAG	16S_F
TAAGGTTCTTCGCGTTGCTT	16S_R
CATATTCGAAGTGCCATTGC	*lmo2230*_F
CTGAACTAGGTGAATAAGACAAAC	*lmo2230*_R
CCTAAACTTGGATTTCCGACTTATCTT	sreB_F
TTCTTATCACGAAAGGTGGAGGG	sreB_R
GGGTACTAGCTGACGGAATTTTATC	*lmo0596*_F
CCCACATACCGAAAAGTAATACGAG	*lmo0596*_R